Multiscale and Multidisciplinary Modeling, Experiments and Design (2025) 8:375
https://doi.org/10.1007/s41939-025-00962-5

ORIGINAL PAPER

Enhancement of heat transfer performance of water-based hybrid nanofluids in an alternate oval tube: a CFD approach

Venkata Ramana Menda[1] · G. Premkumar[2] · Ramu Garugubilli[3] · Ganapathi Sundarapalli[4] · Javed Syed[5]

Received: 5 April 2025 / Accepted: 25 June 2025

Abstract

The alternate oval tube heat exchanger (AOTHe) showcases a groundbreaking approach in chemical processing, focusing on enhancing heat transfer efficiency while reducing pressure loss. This design is evaluated through a numerical analysis of hybrid nanofluids known for their exceptional thermal conductivity and stability. The AOTHe functions effectively within a Reynolds number spectrum of 200–2200, typical of industrial heat exchangers, highlighting the study's relevance. The hybrid nanofluid is also kept at 35 °C, 45 °C and 55 °C. The concentrations of water-based Al_2O_3 + CuO and Al_2O_3 + MWCNT are used to create hybrid nanofluids: 0.01vol%, 0.02vol%, and 0.03vol%. The analysis indicates that transition length and inlet temperature significantly influence performance in a parallel flow system. The presence of secondary flows caused by oval tube axial vortices improves heat transfer efficiency. The results show that the overall heat transfer coefficient is higher with Al_2O_3 + MWCNT hybrid nanofluids than with Al_2O_3 + CuO hybrid nanofluids. Also, the heat transfer enhancement factor (η_{hnf}) is observed for Al_2O_3 + CuO and Al_2O_3 + MWCNTs, ranging from 1.68–2.09 and 1.79–2.92, respectively. Al_2O_3 + CuO performs better at lower temperatures due to its metallic properties, while Al_2O_3 + MWCNT exhibits superior performance due to its high aspect ratio and thermal conductivity.

Keywords Alternate oval tube · Hybrid nanofluids · Effect of transition length · Enhancement factor · Numerical model

1 Introduction

Recent studies have focused on how active and passive components might enhance heat transfer in heat exchangers, especially when elliptical oval tubes are employed in alternating orientations. Also, applications in sectors like oil and gas have resulted from these investigations. Experimental and computational approaches have been investigated to improve heat transfer efficiency and performance. The study focuses on engineering applications, specifically the design of concentric tubes with porous substrates to evaluate heat exchanger performance in counter and parallel flow configurations. It finds that incorporating a porous substrate significantly improves heat exchanger efficiency. Additionally, the research analyzes the impact of the Reynolds number, which indicates the flow regime within the tube, on relevant transient components while varying the flow arrangements of the heat exchanger (Estel et al. 2000). The tube-in-tube heat exchanger shows improved effectiveness, ranging from 40 to 100% better than traditional designs, despite experiencing significant pressure drops. This improvement is due to the innovative oval tube design arranged in alternating directions.

✉ G. Premkumar
pgarapat@gitam.edu

Venkata Ramana Menda
mvramana6028@gmail.com

Ramu Garugubilli
ram.garugubilli@gmail.com

Ganapathi Sundarapalli
ganeshsundarapalli27@gmail.com

Javed Syed
jjaffer@kku.edu.sa

[1] Mechanical Engineering, Aditya Institute of Technology and Management, Tekkali, India

[2] Mechanical Engineering, GITAM Deemed To Be University, Visakhapatnam, India

[3] Department of Mechanical Engineering, Avanthi Institute of Engineering and Technology, Vizianagaram, India

[4] Mechanical Engineering, Aditya University, Surampalem, India

[5] Department of Mechanical Engineering, King Khalid University, 61421 Abha, Saudi Arabia

Published online: 08 July 2025

(Chen et al. 2004, 2006). It is perceived from the experimental studies that elliptical tubes with the passive technique known as a swirl flow generator have shown a substantial improvement of 130% in terms of Nusselt number and a significant drop in pressure drop (Akpinar and Bicer 2005; Wang et al. 2006). The thermal efficiency of shell and tube heat exchangers utilizing CuO-ZnO/water hybrid nanofluid and various tube geometries has been studied. It is perceived that the hexagonal tubes enhanced heat transfer rates by 22.11% over round tubes and 18.42% over elliptical tubes, with coefficients rising alongside fluid velocity (Behera et al. 2024). The performance of a tube-in-tube heat exchanger, utilising a semi-circular plate insert to enhance turbulence, is intricately linked to its overall heat transfer efficiency (Kumar et al. 2006).

Green synthesising hybrid nanofluids prepared using graphene have been explored to enhance thermal performance in flat-plate solar collectors. Utilizing clove-treated carbon nanotubes and titanium dioxide, the research demonstrates significant improvements in energy and exergy efficiency, achieving optimal results at specific concentrations and flow rates, while reducing solar collector size (Alfellag et al. 2024). Research has focused on the dispersion of nanoparticles like graphene and multi-walled carbon nanotubes (MWCNTs) in base fluids and oils. Studies on oval tube designs and heat transfer indicate that corrugated tubes improve heat transfer in turbulent flow, whereas smooth tubes are less effective. These findings have significant practical implications for the design and operation of heat exchangers, particularly in industries where heat transfer efficiency is a critical factor. Researchers are focusing on enhancing the performance and cost-effectiveness of heat exchangers by analyzing alternating flattened tube flow, which shows promising economic advantages over traditional circular tubes. While this approach offers potential benefits, it is crucial to recognize the limitations of oval pipe designs, particularly concerning higher pressure drops compared to circular tubes. Understanding these challenges can aid professionals in mechanical engineering and thermal sciences in their future work (Sajadi et al. 2016, 2017; Vaezi et al. 2017; Rennie and Raghavan 2006). The key findings are that altering pitch length and aspect ratio can enhance performance, while new designs, such as oval tubes, demonstrate lower pressure drops than traditional round tubes. However, a significant research gap exists in the long-term performance analysis of these innovative designs, particularly regarding their durability and efficiency over extended periods. Additionally, while various techniques have been explored to optimize hybrid solutions and mixed reaction processes, there is a need for further investigation into the stability and effectiveness of these approaches in practical applications (Tan et al. 2013; Taler and Ocłoń 2014; Liu et al. 2020; Ghasemi et al. 2021; Nagaraju et al. 2024; Insiat Islam et al. 2023). Moreover, comprehensive numerical investigations related to passive techniques and oval tube heat exchangers are represented in Table 1.

1.1 Objective of the work

The need for further study on non-circular tube heat exchangers, specifically AOTHe, is underscored by the promising thermal performance improvements observed in recent research involving oval and elliptical geometries. However, a significant research gap exists in the exploration of hybrid nanofluids within these complex geometrical systems, as most existing studies have focused on single phase nanofluids, often relying on simplified hydraulic diameter assumptions that may not accurately reflect the unique characteristics of AOTHe. This limitation raises potential problems in evaluating heat transfer enhancement and system performance, as current assessments frequently overlook critical factors such as pumping power requirements and comprehensive system-level metrics. This innovative research could significantly advance the understanding and optimization of hybrid nanofluids in advanced heat transfer applications.

The research highlights the importance of the design parameters, such as spacing, arrangement, aspect ratio, and enhancement ratio, in optimizing the performance of AOTHe. However, it identifies a gap in the existing literature regarding the reliance on experimental evidence for design, which is labour-intensive. The proposed numerical model aims to fill this gap by facilitating parametric research, suggesting a need to explore further its effectiveness in streamlining the design process and improving heat exchanger performance. The novelty of the present work is that the transition length in alternating oval tube heat exchangers affects flow dynamics, boundary layer development, and heat transfer efficiency, affecting hybrid nanofluid thermal performance. Maximizing heat exchange and minimizing pressure decreases requires optimizing this length. Thermally active hybrid nanofluids interact with the transition area to increase heat transfer coefficients and Nusselt numbers, lowering thermal resistance. A shorter transition length may thin boundary layers and increase heat flow, but it may cause localized overheating. A longer duration may increase pressure decreases. Key relationships between transition length and thermal characteristics guide optimization. To achieve this, the present work is to analyze the effect of oval tube transition lengths (4 mm, 5 mm, 6 mm) in a double-pipe heat exchanger on the performance of hybrid nanofluids (Al_2O_3 in CuO and MWCNT) at varying concentrations. The study will first validate experimental results

Table 1 Various heat exchangers reveal significant findings

Refs.	Analysis	Re range	Review aspect
Chen (2007)	Num	$Re_i = 100–2000$, $Re_O = 10–40$	The wall temperature in a heat exchanger changes along both axial and circumferential pipe directions, contrasting with the previous studies' distribution
Chen and Dung (2008)	Num	Re = 100–2000	It is suggested that an oval tube as an inner pipe in a double-pipe heat exchanger can significantly enhance performance by forming axial vortices
Cheng et al. (2017)	Exp	Re = 4000–30000	At higher flow rates, twisted oval tube heat exchangers perform better
Vaezi et al. (2017)	Num	Re = 100–1600	Regardless of the aspect ratio and Reynolds number, heat transfer is greatly improved when an oval alternating tube is used as the inner pipe in a double-pipe heat exchanger
Unger et al. (2020)	Exp	Re = 1800–7800	The fin-tube heat exchanger was tested at various tilt angles to enhance conduction and convection modes, revealing the optimal range as 0° to 40° horizontal
Gholami et al. (2019)	Num	Re = 500–5000	The study reveals that corrugated profiles with fins improve heat transfer efficiency in finned tube heat exchangers (FTCHEs) compared to traditional fins and oval tubes, with η-factor improvements
Gholami et al. (2017)	Num	Re = 200–900	According to case studies, an oval tube compact heat exchanger with one or three corrugated fins shows an improvement between 5 and 15%
Du et al. (2014)	Exp	Re = 1300–13000	Its angle and design greatly influence the heat transfer efficiency of an oval-tube heat exchanger with two fins
Chu et al. (2009)	Num	Re = 500–2500	An oval tube heat exchanger with a longitudinal vortex generator and three-row fins has a noticeably higher Nusselt number
Tan et al. (2013)	Num	Re = 5000–25000	To identify the best model for evaluating pertinent parameters, the research examines how different turbulence models affect heat transfer and adds a heat transfer enhancement factor
Taler and Ocłoń (2014)	Num	Re = [150–400] and [4000–12000]	Higher aspect ratios positively impact the Nusselt number in heat exchangers, although numerical data may underestimate its value by 13
Tiwari et al. (2003)	Num	Re = 1000	The study found that using oval tubes and delta winglet-type vortex generators in rectangular channels significantly improves heat transfer by 43.86% when arranged in staggered mode
Herpe et al. (2009)	Num	Re = 300	The analysis indicates that fin efficiency increases constantly in the fluid field as entropy generation decreases

(Nagaraju et al. 2023) from existing literature with a numerical model, which will then be used to predict the performance of the heat exchanger under parallel flow arrangements and varying temperatures (35–55 °C) of the hybrid nanofluid. Key metrics such as overall heat transfer coefficient, heat transfer enhancement factor, and performance index are analysed.

2 Methodology

2.1 Properties of nanofluid

The analysis is pertinent to verify the influence of *TL* of AOTHe on the performance of different hybrid nanofluids.

Table 2 Thermophysical properties of nanoparticles (Mohammad et al. 2022; Elshazly et al. 2023)

Properties	Water	Al_2O_3	CuO	MWCNT
ρ (kg/m^3)	997.05	3970	6350	2100
k (W/m K)	0.606	40	69	3000
Cp (J/kg K)	4181.3	765	535.6	519
υ (Ns/m^2)	0.00089	–	–	

The water-based hybrid nanofluids are proposed by dispersing Al_2O_3 in CuO and MWCNT separately at concentrations of 0.01%, 0.02% and 0.03%. The inlet temperature to AOTHe is considered from 35 °C to 55 °C by treating a single-phase mixture at a steady state. The properties of these materials are referred to in the literature and presented in Table 2. Eventually, the thermophysical properties of the hybrid nanofluid are calculated using correlations available in the literature (Sahu et al. 2020) i.e., Eq. (1–6).

The present work uses Al_2O_3 + MWCNT and Al_2O_3 + CuO hybrid nanofluids as the working fluids, consisting of a suspension of these nanoparticles in the base fluid according to the mixture rules. The current thermal hydrodynamic study involves two distinct mixtures: Al_2O_3 combined with MWCNT and Al_2O_3 combined with CuO nanoparticles, referred to as hybrid nanoparticles. The thermal and electrical conductivity of Al_2O_3 is generally lower than that of MWCNT. Al_2O_3 exhibits lower conductivities in comparison to MWCNT. The hybrid preparation of MWCNT and Al_2O_3 nanoparticles results in enhanced conductivities that significantly exceed those of the base liquid. The flow of hybrid nanofluids in heat exchanger devices represents a relatively new study area. Consequently, additional research is necessary to enhance understanding, which is essential for practical applications [45]. The selection of Al_2O_3 as a dispersion material in MWCNT and the incorporation of Al_2O_3 provide superior chemical stability and oxidation resistance, thereby safeguarding MWCNTs in corrosive environments found in heat exchangers. Also, Al_2O_3 nanoparticles enhance wettability and dispersion in base fluids, thereby improving thermal performance. Similarly, combining CuO and Al_2O_3 results in a hybrid nanofluid that exhibits improved thermal conductivity properties. CuO exhibits a higher density, which may present challenges regarding stability in fluid environments. The incorporation of Al_2O_3 enhances the overall density of the nanofluid, thereby improving its stability. Additionally, Al_2O_3 nanoparticles possess a high surface area, facilitating enhanced interaction with the fluid and improving heat transfer efficiency. Therefore, the motivation behind using Al_2O_3-water hybrid nanofluid as the working fluid for this study was driven by this motivation. The following correlations, Eq. (1–6), are referred from literature (Sahu et al. 2020; Khanafer and Vafai 2011; Abed et al. 2020).

$$\rho_{hnf} = (1 - \varnothing_1 - \varnothing_2)\rho_{bf} + \varnothing_1\rho_1 + \varnothing_2\rho_2 \tag{1}$$

$$(\rho Cp)_{hnf} = (1 - \varnothing_1 - \varnothing_2)\left(\rho C_p\right)_{bf} + \varnothing_1 + (\rho Cp)_1 + \varnothing_2(\rho Cp)_2 \tag{2}$$

$$k_{snf} = 0.25[(3\varnothing - 1)k_p + (2 - 3\varnothing)k_{bf} + \sqrt{\Delta} \tag{3}$$

where, $\Delta = [(3\varnothing - 1)k_{np} + (2 - 3\varnothing)k_{bf}]^2 + 8k_{np}k_{bf}$

$$k_{hnf} = \frac{1}{\varnothing}\sum_{i=1}^{n}(\varnothing_i k_{nf,i}) where \sum_{i=1}^{n}\varnothing_i \tag{4}$$

$$\mu_{snf} = \mu_{bf}\left(1 + 7.3\varnothing + 123\varnothing^2\right) \tag{5}$$

$$\mu_{hnf} = \frac{1}{\varnothing}\sum_{i=1}^{n}(\varnothing_i \mu_{nf,i}) \text{where} \sum_{i=1}^{n}\varnothing_i \tag{6}$$

The present considers a binary hybrid nanofluid, i.e., n = 2.

2.2 Modelling and meshing of AOTHe

The computational domain is an alternative oval tube as an inner tube, and the outer tube is circularly oriented axially. The schematic representation of the geometry modelled in Space claim *TL*-1, *TL*-2, and *TL-3* represents *TL* values of 4 mm, 5 mm and 6 mm, respectively. The dimensions are presented in Table 3; the inner tube, i.e., AOTHe, receives a hybrid nanofluid at different inlet temperatures, and the outer tube receives water at 30 °C. The heat exchanger mode is parallel in both inner and outer fluid directions. Subsequently, the model is imported into ICEM-CFD to generate an unstructured mesh of AOTHe for various *TL*s. The 3D computational domain's mesh generation utilizes ICEM CFD's unique features, generating high-quality unstructured meshes for complex geometries and highlighting alternate oval tubes. Figure 1 shows the computational domain of AOTHe with *TL*-5 mm and its mesh. A systematic approach for mesh generation includes surface and volume meshing, boundary layer refinement, and quality assessment. The procedure guarantees superior mesh quality, thereby improving computational accuracy and efficiency. The unstructured and hybrid meshes allow for the development of hexahedral, tetrahedral, and

Table 3 Dimensional parameters of AOTHe

Alternate direction oval tube	Dimensions
Circular pipe diameter (d_i)	16.5 mm
Oval tube major axis (l_j)	25 mm
Oval tube minor axis (l_m)	13.5 mm
Length of oval tube (L)	25 mm
Outer tube diameter (d_o)	33 mm
Length of heat exchanger	1060 mm
Transition length (TL)	5 mm
Pipe material	Copper
Thermal conductivity of copper	380 W/m K
Density of copper	8960 kg/m^3

prism-based control volumes designed explicitly for complex geometries. The generated mesh can be efficiently exported to CFD solvers, establishing control volumes for Finite Volume Method (FVM) computations, as shown in Fig. 1. Local refinement and quality control measures, such as skewness and aspect ratio checks, improve the accuracy and stability of numerical simulations by enhancing control volume quality. The mesh quality is verified in terms of skewness. Firstly, a default mesh is generated, and a high-quality unstructured surface mesh utilises triangular or quadrilateral elements, incorporating global and local refinements. Delaunay triangulation generates tetrahedral elements, and prism layers are incorporated adjacent to walls to resolve boundary layers effectively. The final computational mesh for the analysis is obtained by conducting a grid independence study.

The objective of the numerical investigation is to analyze the performance of an AOTHe using different nanofluids under steady-state conditions, focusing on the effects of varying Reynolds numbers (200–2200) and mass flow rates of hybrid nanofluids while keeping the outer tube fluid (water) at a constant Reynolds number of 1000 and temperature of 28 °C. The inlet temperature of the inner fluid varies from 35 to 55 °C.

2.3 Numerical modelling

The governing equations of the computational domain, which operate under steady flow conditions, are solved using the finite volume approach implemented in FLUENT software. The equations encompass mass, momentum,

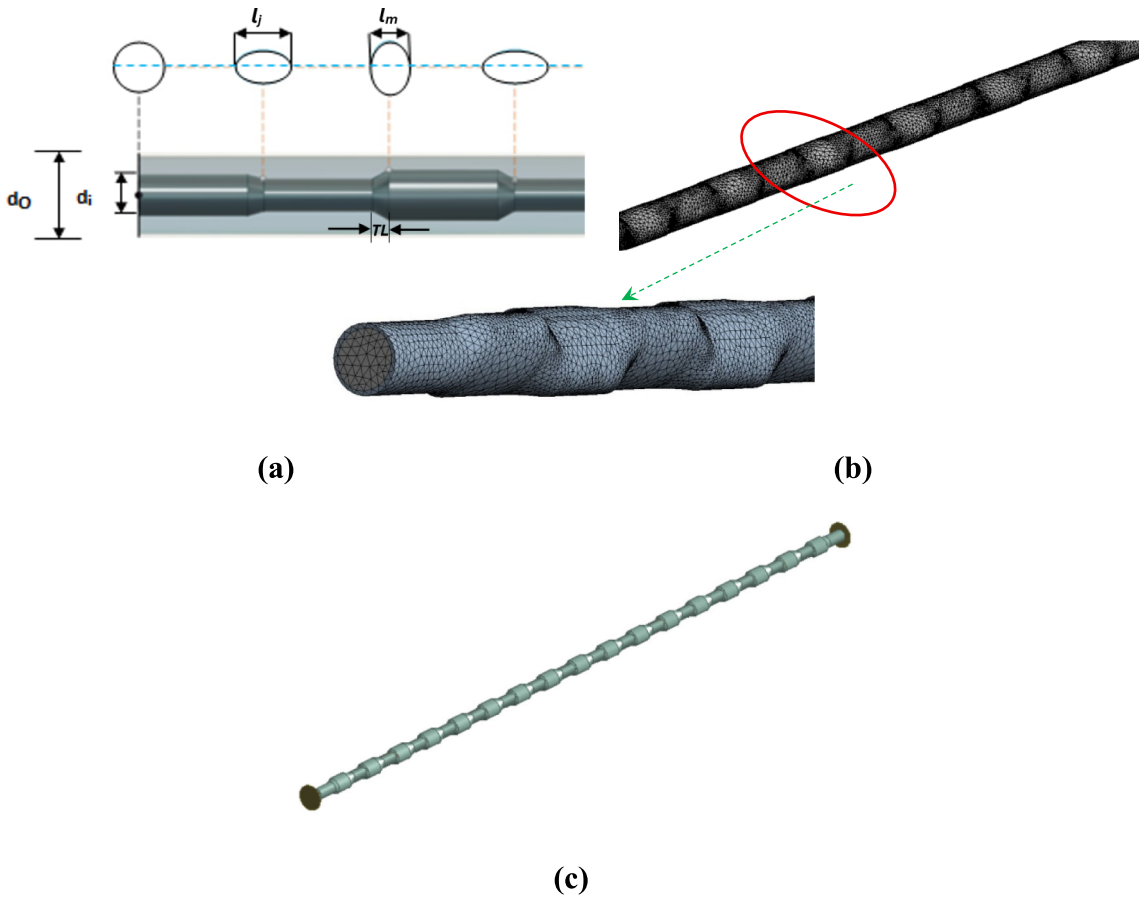

Fig. 1 **a** Geometry of AOTHe with different TL 5 mm **b** Meshing of AOTHe with TL 5 mm **c** Geometry model of TL-5 mm AOTHe

and energy variables. The second-order upwind approach balances numerical stability and accuracy in advection-dominated simulations. SIMPLE algorithm is employed to tackle the continuity and momentum equations. A technique that uses pressure and consistent conditions tackles the governing equations. In order to investigate numerical simulations, a boundary condition on the mass flow rate at a certain input temperature for the nanofluid must be implemented. The computational grid's unstructured form is discretised and developed along the inner alternative oval tube. The enhanced wall treatment accurately depicts the near-wall boundary layer during the simulations. The leading governing and turbulence modelling equations are from Eq. (7–11).

$$\frac{\partial \rho}{\partial t} + \frac{(\rho u_j)}{X_j} = 0 \tag{7}$$

$$\rho \frac{\partial u_i}{\partial t} + \rho u_j \frac{\partial u_i}{\partial x_j} = -\frac{\partial P}{\partial x_i} + \mu \frac{\partial}{\partial x_j}\left(\frac{\partial u_i}{\partial x_j} + \frac{\partial u_j}{\partial x_i}\right) \tag{8}$$

$$\rho \frac{\partial T}{\partial t} + \rho \frac{\partial u_i T}{\partial t} = -P \frac{\partial u_i}{\partial x_i} + k \frac{\partial}{\partial x_j}\left(\frac{\partial u_i}{\partial x_j} + \frac{\partial u_j}{\partial x_i}\right) \tag{9}$$

The k-ε model has been used for simulating turbulent flow, and the associated equations are given below.

$$\frac{\partial}{\partial t}(k) + \frac{\partial}{\partial x_i}(k u_i) = \frac{\partial}{\partial x_i}\left(v + \frac{v_t}{\sigma_k}\right)\frac{\partial k}{\partial x_j} + P_k - \in \tag{10}$$

$$\frac{\partial}{\partial t}(\in) + \frac{\partial}{\partial x_i}(\in u_i) = \frac{\partial}{\partial x_j}\left(v + \frac{v_t}{\sigma_\in}\right)\frac{\partial \in}{\partial x_j} + C_{1\in}\frac{\in}{k}(P_k) - C_{2\in}\frac{\in^2}{k} \tag{11}$$

where: $\mu_t = \rho C_\mu \frac{k^2}{\epsilon}$, $P_k = -\rho\overline{u_i u_j}\frac{\partial u_j}{\partial x_i}$, $C_{1\epsilon} = 1.44$, $C_{2\epsilon} = 1.92$, $C_\mu = 0.09$, $\sigma_k = 1$, $\sigma_\epsilon = 1.3$

Also, U_o is calculated using Eq. (11).

$$U_o = \frac{Q_{overallheattransfer}}{A_{total,surface}\Delta T_m} \tag{12}$$

where ΔT_m is the logarithmic mean temperature difference (*LMTD*) for parallel flow heat exchanger.

$$\Delta T_m = \frac{\Delta T_1 - \Delta T_2}{ln\frac{\Delta T_1}{\Delta T_2}} \tag{13}$$

Mean temperatures at the inlet and outlet are determined through numerical simulations, while LMTD differences for parallel flow are expressed using conventional methods. Where, ΔT_1 (T_{hi}-T_{ci}) and ΔT_2 (T_{ho} -T_{co}).

The oval tube geometry is designed to minimize boundary layer thickness and improve flow distribution across the tube surface, which enhances convective heat transfer efficiency. The enhancement factor is a key metric that compares heat transfer performance between oval tube heat exchangers and conventional round tube designs under equivalent operating conditions. This factor quantifies the ratio of heat transfer in the modified oval design to that of the standard design, serving as a critical measure for engineers to evaluate the feasibility of alternative geometries in design applications. Understanding the enhancement factor (η_{hnf}) is essential for optimizing designs to balance heat transfer efficiency and minimise pressure drops. With compact profiles, oval tubes can potentially maintain or improve heat transfer performance while addressing space and weight constraints. This makes them a viable option for applications where traditional designs may not suffice.

The heat transfer enhancement factor (η_{hnf}) of hybrid nanofluid is estimated using (Chen and Dung 2008),

$$\eta_{hnf} = \frac{U_{AOTHe}}{U_{Circular}} \tag{14}$$

The pumping power (P_{hnf}) of the hybrid nanofluids can be estimated using correlation (Saleh and Sundar 2021),

$$P_{hnf} = \left(\frac{\dot{m}_{hnf}}{\rho_{hnf}}\right) \times \Delta p_{hnf} \tag{15}$$

Similarly, the friction factor of hybrid nanofluid is calculated using Eq. (16) (Syam Sundar et al. 2020),

$$f_{nf} = \frac{\Delta p_{nf}}{\left(\frac{L_p}{D_h}\right)\left(\frac{\rho_{nf} v^2}{2}\right)} \tag{16}$$

Moreover, the performance index ratio(η_{PI}) is predicted using correlation (Tiwari et al. 2013),

$$\eta_{PI} = \frac{\left[\frac{\dot{Q}_{avg}}{P_{hnf}}\right]_{hnf}}{\left[\frac{\dot{Q}_{avg}}{P_{bf}}\right]_{bf}} \tag{17}$$

3 Results and discussions

3.1 Validation

The comparison of heat transfer enhancement using alternate oval tube heat exchanger has been done by analysing experimental data (Nagaraju et al. 2023) and numerical predictions of the Nusselt number at various Reynolds numbers. The numerical simulations analysed three fluids considered in the experimental investigation: water and water/graphene nanofluids, i.e., G0.1% and G0.2%. Experimental data were validated through comparison with CFD simulations,

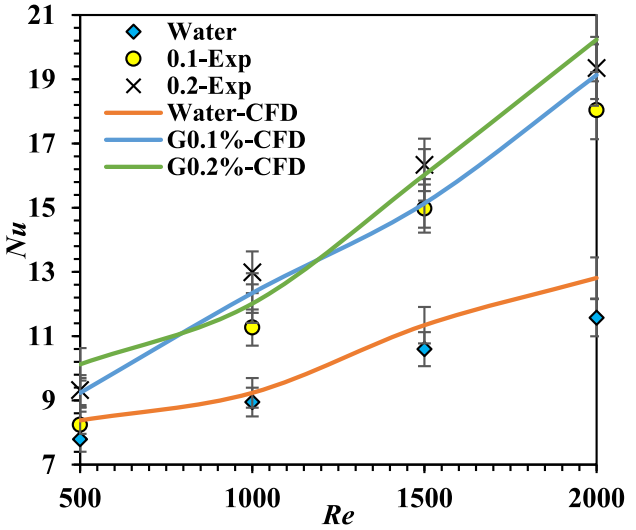

Fig. 2 Validation of alternate oval tube performance using water/graphene nanofluids

where deviations were quantified, and trends were analysed. Figure 2 illustrates the relationship between the average Nusselt number and the inlet velocity of heat transfer fluid. The results strongly agree with the current body of literature, indicating a mean percentage error of 7.09%, 7.28%, and 5.63% for water, G0.1%, and G0.2%, respectively. The error is anticipated to fluctuate concerning Reynolds number and nanoparticle concentration. The quantification of these errors offers a detailed understanding of model accuracy. The observed trends indicate that CFD is an effective tool for modelling heat transfer phenomena; however, discrepancies may occur due to idealised boundary conditions or assumptions inherent in the numerical model.

The grid independence test creates three distinct unstructured meshes with skewness values of 0.65, 0.82, and 0.84, respectively, and corresponding mesh elements range from 912,890 to 997,304. The corresponding outlet temperature of nanofluid is 32.05 °C, 31.65 °C and 31.92 °C, respectively. To maintain a Reynolds number of 1000 for the inner and outer tubes, numerical simulations are performed using an inner fluid input temperature of 35 °C and an outer tube temperature. The analysis yields the mass-weighted average outlet temperature, and further mesh refinement is considered minimal significance.

3.2 Effect of hybrid nanofluid inlet temperature

The effect of the inlet temperature of the inner tube on the overall heat transfer coefficient of AOTHe is presented for *TL*-5 mm in Fig. 3. The inner tube inlet temperature plays a significant role in influencing the U_o while employing hybrid nanofluids, such as Al_2O_3 + CuO (AC0.01%, AC0.02% and AC0.03%) and Al_2O_3 + MWCNT (AM0.01%, AM0.02% and AM0.03%), at various volume concentrations. Hybrid nanofluids enhance thermal properties due to the synergistic effects of their components, offering higher thermal conductivity and heat transfer performance compared to base fluids or single nanofluids. Figure 3a illustrates that the total heat transfer coefficient slightly increases at an input temperature of 35 °C because of reduced thermal agitation.

Heat transfer performance shows a noticeable improvement as the concentration increases from 0.01% to 0.03%. Al_2O_3 + CuO performs slightly better at lower temperatures due to its metallic properties, which enhance heat conduction. At 45 °C, the heat transfer coefficient increases significantly compared to performance at 35 °C, as depicted in Fig. 3b. The temperature rise intensifies hybrid nanofluids' Brownian motion and thermophysical properties, leading to better convective heat transfer. Al_2O_3 + MWCNT, owing to its high aspect ratio and thermal conductivity, exhibits superior performance compared to Al_2O_3 + CuO, especially at higher concentrations. The enhanced dispersion of hybrid nanoparticles, which results in better thermal conductivity, causes higher thermal performance at 55 °C, as shown in Fig. 3c. The temperature difference between the inner tube and the fluid enhances convective heat transfer. However, excessive temperature can lead to minor instability in nanoparticle suspension, slightly affecting performance. Al_2O_3 + MWCNT continues to demonstrate better results at all concentrations, attributed to its unique tubular structure and ability to form thermally conductive networks. Both nanofluids show a direct relationship between inlet temperature and heat transfer coefficient, improving performance at higher concentrations and temperatures. Al_2O_3 + MWCNT exhibits superior heat transfer capability due to its advanced thermal properties and structural advantages.

The heat transfer enhancement factor (η_{hnf}) quantifies the improvement in heat transfer performance compared to the base fluid, highlighting the combined influence of nanoparticle properties and operational conditions. As shown in Fig. 4a for TL-5 mm AOTHe, the η_{hnf} is comparatively low at an input temperature of 35 °C because there is less thermal energy available for nanoparticle activity.

The contribution of Brownian motion and particle–fluid interactions is minimal at this temperature. As the volume concentration increases, the η_{hnf} improves, with Al_2O_3 + CuO showing better performance due to its metallic nanoparticles' higher thermal conductivity, which dominates under lower thermal gradients. At 45 °C, the η_{hnf} increases substantially for both hybrid nanofluids, as presented in Fig. 4b. The elevated temperature enhances nanoparticle dispersion and thermal energy transfer, improving convective heat transfer rates. At this intermediate temperature, Al_2O_3 + MWCNT begins to outperform Al_2O_3 + CuO due to the superior thermal conductivity of MWCNTs and the ability to form effective thermal networks. Higher concentrations (0.02%

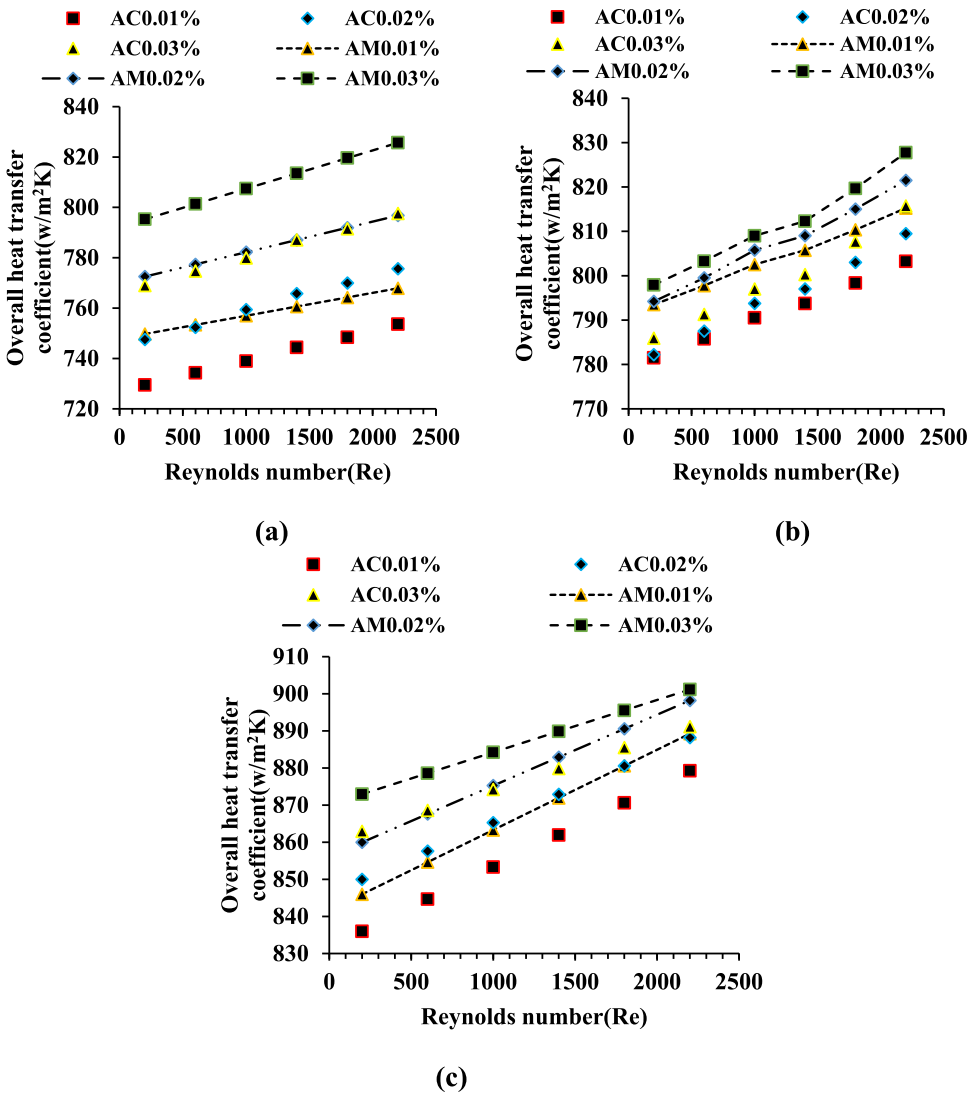

Fig. 3 Variation of overall heat transfer coefficient for different hybrid nanofluid volume concentrations at **a** 35 °C **b** 45 °C **c** 55 °C temperature

and 0.03%) yield greater enhancements, highlighting the synergistic effect of temperature and concentration. At 55 °C, the η_{hnf} attains its maximum value. Increased inlet temperature intensifies Brownian motion and decreases fluid viscosity, improving heat transfer efficiency.

Al_2O_3 combined with MWCNT exhibits the highest heat transfer efficiency (η_{hnf}) at a concentration of 0.03%, owing to MWCNTs' superior thermal conductivity and surface area. While Al_2O_3 + CuO shows satisfactory performance, it is less effective than Al_2O_3 + MWCNT due to inferior heat transport mechanisms. Both hybrid nanofluids demonstrate increased η_{hnf} with higher inlet temperatures and concentrations. The inlet temperature affects the performance index (ηPI), showing moderate enhancement at 35 °C and improving with lower viscosity. Al_2O_3 + CuO benefits from lower concentrations, while Al_2O_3 + MWCNT performs better at 45 °C.

3.3 Effect of TL

The transition length (TL) in an alternative elliptical axis oval tube heat exchanger significantly influences the overall heat transfer coefficient (U_o) when hybrid nanofluids such as Al_2O_3 + CuO and Al_2O_3 + MWCNT are used at various volume concentrations (0.01%, 0.02%, 0.03%). The *TL* affects flow behaviour, turbulence generation, and heat transfer area, impacting the overall heat transfer coefficient, as shown in Figure. For *TL*-4 mm, the shorter transition length leads to enhanced turbulence near the tube walls, improving convective heat transfer. This configuration maximises local heat transfer but may slightly increase pressure drop. Both nanofluids exhibit a notable rise in U_o, with Al_2O_3 + CuO showing better performance at lower concentrations due to its metallic properties that enhance conduction, as shown in Fig. 5a. However, the shorter *TL* restricts the development of fully turbulent flow, limiting the maximum achievable

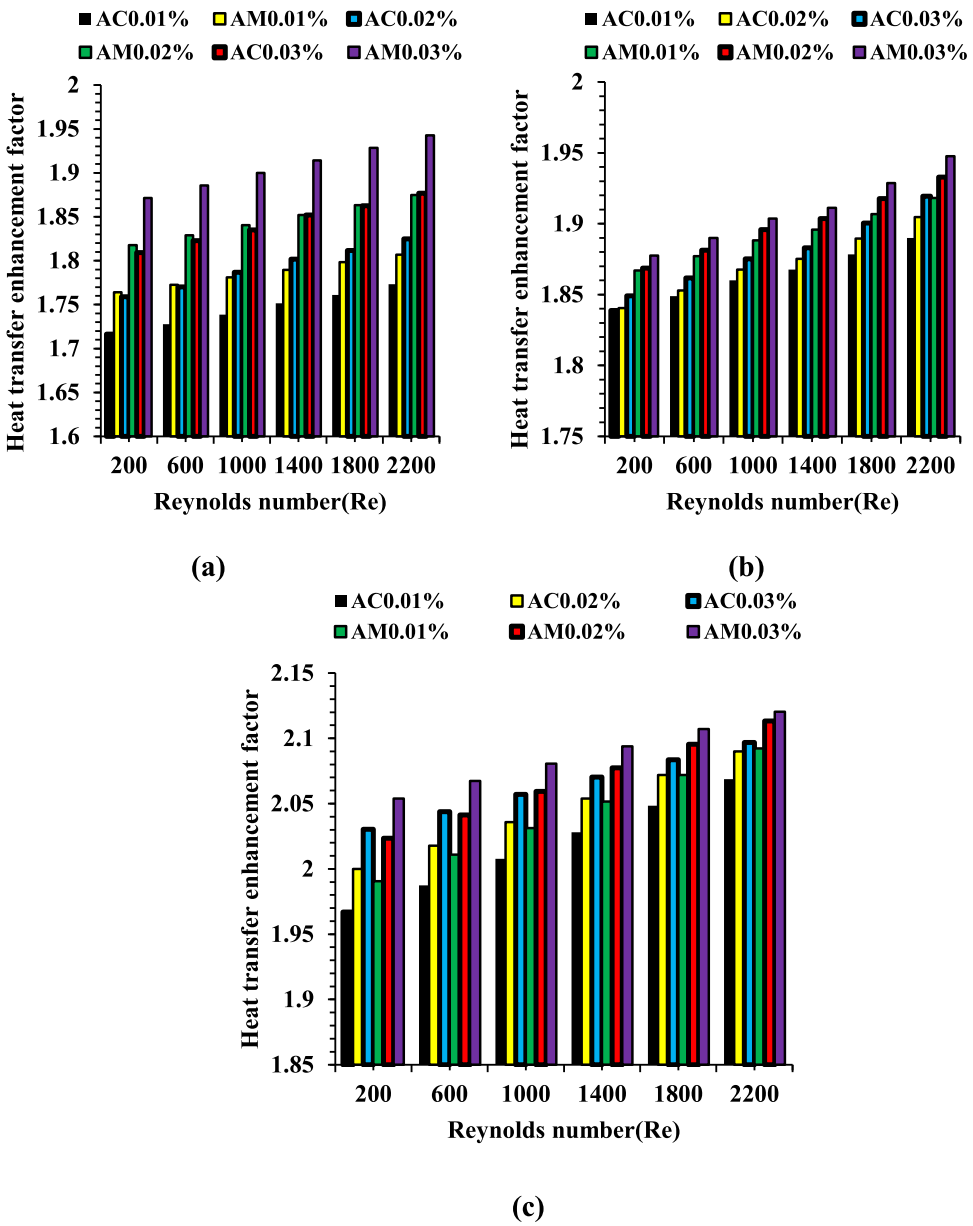

Fig. 4 Variation of heat transfer enhancement factor (η_{hnf}) at various inlet temperatures of hybrid nanofluid **a** 35 °C **b** 45 °C **c** 55 °C

heat transfer enhancement. At *TL*-5 mm, the heat transfer coefficient improves further due to an optimal balance between turbulence generation and flow stabilisation. The increased transition length allows a more uniform distribution of nanoparticles and greater heat exchange. Al_2O_3 + MWCNT outperforms Al_2O_3 + CuO in this case, particularly at higher concentrations (0.02% and 0.03%), as the MWCNTs' high thermal conductivity and network formation further amplify heat transfer. The longer transition length for *TL*-6 mm provides a smoother flow transition, reducing pressure drop and enhancing particle suspension.

However, the reduced turbulence compared to shorter *TL* values slightly limits the convective heat transfer rate, as shown in Fig. 5c. Al_2O_3 + MWCNT continues to demonstrate superior performance due to its ability to sustain higher heat flux under smoother flow conditions. Higher concentrations (0.03%) are particularly effective at this *TL* in maintaining an elevated heat transfer coefficient. Overall, the effect of *TL* on U shows that a moderate *TL* -5 mm offers the best balance between turbulence and flow stability, maximizing heat transfer performance. Al_2O_3 + MWCNT consistently delivers better results across all *TL*s and concentrations due to its advanced thermophysical properties, making it a preferred choice for high-efficiency heat exchanger applications.

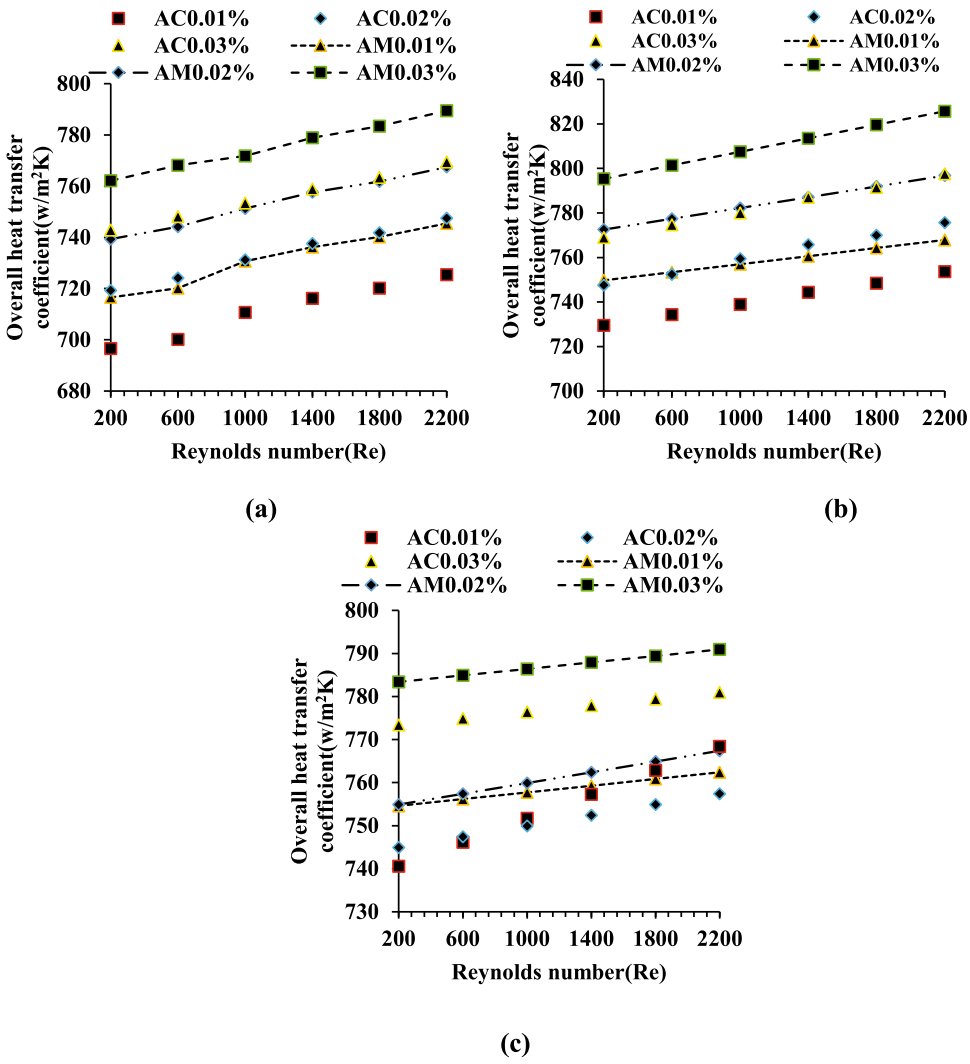

Fig. 5 Variation of overall heat transfer coefficient for different Transition lengths **a** *TL*-4 mm **b** *TL*-5 mm **c** *TL*-6 mm

3.4 Performance index ratio

At a temperature of 35 °C, the η_{PI} demonstrates a moderate enhancement for both hybrid nanofluids, as shown in Fig. 6. The analysis reveals that at reduced temperatures, the viscosity of nanofluids increases, leading to higher pumping power requirements. While heat transfer improves, this is offset by a slight decrease in the performance index due to increased viscosity. Specifically, Al_2O_3 + CuO shows better at lower concentrations (0.01%) due to its metallic properties that enhance conduction with minimal viscosity increases. At reduced temperatures, the viscosity of nanofluids increases, leading to higher pumping power requirements. While heat transfer improves, the performance index slightly decreases due to this increased viscosity. The nanofluid composed of Al_2O_3 + CuO performs better at lower concentrations (0.01%) because its metallic properties enhance conduction with minimal viscosity increase. At 45 °C, the performance indicator improves significantly due to better heat transfer efficiency and lower viscosity. The higher temperature boosts nanoparticle mobility through Brownian motion, enhancing thermal conductivity, especially for the Al_2O_3 + MWCNT hybrid nanofluid. This hybrid demonstrates a superior performance index compared to Al_2O_3 + CuO, particularly at higher concentrations (0.02% and 0.03%), as the network-forming characteristics of MWCNTs improve thermal conductivity while keeping viscosity manageable. The study concludes that the combination of Al_2O_3 and MWCNT yields the highest performance index for heat transfer enhancement, particularly at a concentration of 0.03%, due to improved thermal conductivity and particle dispersion.

This formulation maintains an acceptable pressure drop and demonstrates superior thermal performance when compared to Al_2O_3 combined with CuO, which is less efficient at elevated temperatures and concentrations. The performance

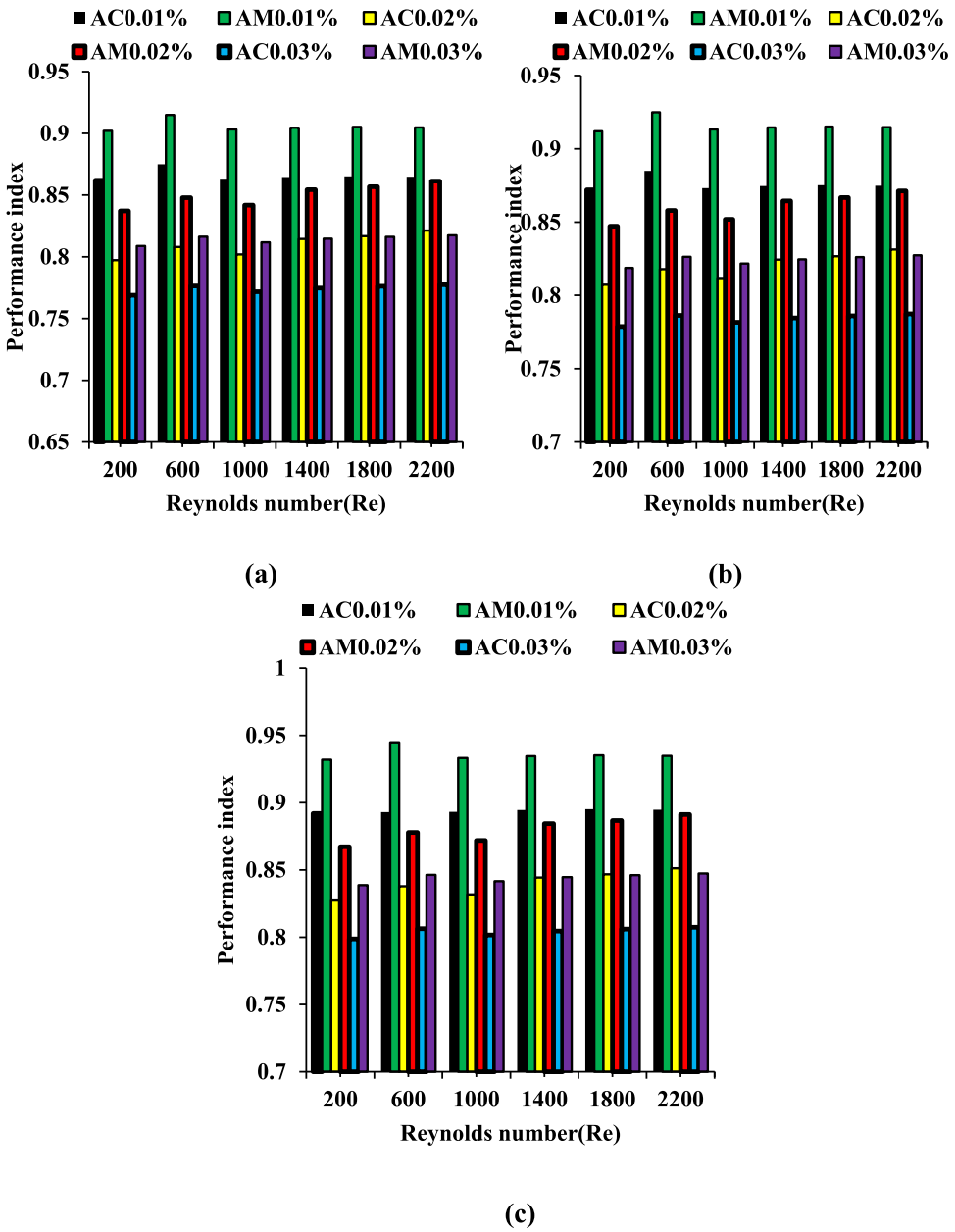

Fig. 6 Effect of inner tube inlet temperature on the performance index at different hybrid nanofluid volume concentrations **a** 35 °C **b** 45 °C **c** 55 °C

index exhibits an upward trend with increasing inlet temperatures for both hybrid nanofluids. Al_2O_3 and MWCNT are identified as the optimal selections for high-performance heat exchanger applications.

4 Conclusions

The study investigates the performance of an alternate oval tube heat exchanger (AOTHe) operating with hybrid nanofluids from Al_2O_3, CuO, and MWCNTs at different volumetric concentrations. Validating experimental data establishes the numerical mode, and the computational domain has a double-pipe design. The outside part of this arrangement is a circular water-transporting pipe, while the inner part is an oval tube directed in a different direction. The research investigates how to change the Reynolds number, input temperature, TL and *Uo*, and *HEf*. The inner tube has an inlet temperature that significantly impacts the overall heat transfer coefficient of AOTHe when utilising hybrid nanofluids such as Al_2O_3 + CuO and Al_2O_3 + MWCNT.

- Hybrid nanofluids improve thermal properties by providing increased thermal conductivity and enhanced heat transfer performance. The combination of Al_2O_3 and CuO

demonstrates enhanced performance at reduced temperatures, attributable to its metallic characteristics. In contrast, the Al_2O_3 and MWCNT composite shows improved performance owing to its elevated aspect ratio and thermal conductivity.

- The inlet temperature of the inner tube significantly impacts the overall heat transfer coefficient when using hybrid nanofluids. Higher temperatures and concentrations enhance thermal performance, with Al_2O_3 + MWCNT consistently outperforming Al_2O_3 + CuO. Optimal conditions improve heat transfer efficiency, demonstrating the importance of selecting appropriate nanofluids for thermal applications.
- The increase in overall heat transfer coefficient was approximately 9.15%, 14.48% and 6.04% for TL = 4 mm, 5 mm, and 6 mm, respectively. This trend indicates that the hybrid nanoparticle composition and transition length significantly affect heat transfer performance. The configuration with a transition length of 5 mm exhibited the highest thermal enhancement, indicating an optimal balance between flow development and thermal boundary layer growth.

Acknowledgements The author extends their appreciation to the Deanship of Research and Graduate Studies at King Khalid University for funding this work through a Large Research Project under grant number RGP2/526/46.

Author contributions V R M: Visualization; P G: Conception, study design, execution, acquisition of data; R G: Visualization; G S: analysis and interpretation; J S: Funding, reviewing.

Funding Deanship of Scientific Research, King Khalid University, RGP2/526/46.

Availability of data and material No datasets were generated or analysed during the current study.

Declarations

Conflict of interest The authors declare no competing interests.

Ethical approval This article contains no studies with human participants or animals performed by authors.

Consent to participate All co-workers have agreed to participate.

Consent for publication All co-workers have agreed to publication.

References

Abed N, Afgan I, Cioncolini A, Iacovides H, Nasser A, Mekhail T (2020) Thermal performance evaluation of various nanofluids with non-uniform heating for parabolic trough collectors. Case Stud Therm Eng 22:100769. https://doi.org/10.1016/j.csite.2020.100769

Akpinar EK, Bicer Y (2005) Investigation of heat transfer and exergy loss in a concentric double pipe exchanger equipped with swirl generators. Int J Therm Sci 44:598–607. https://doi.org/10.1016/j.ijthermalsci.2004.11.001

Alfellag MA, Mohamed Kamar H, Abidin U, Kazi SN, Alawi OA, Muhsan AS et al (2024) Green synthesized clove-treated carbon nanotubes/titanium dioxide hybrid nanofluids for enhancing flat-plate solar collector performance. Appl Therm Eng 246:122982. https://doi.org/10.1016/J.APPLTHERMALENG.2024.122982

Behera M, Nayak J, Bal S (2024) Heat transfer analysis of CuO-ZnO/water hybrid nanofluid in a Shell and tube heat exchanger with various tube shapes. Int J Thermofluids 24:100972. https://doi.org/10.1016/J.IJFT.2024.100972

Chen WL (2007) A numerical study on the heat-transfer characteristics of an array of alternating horizontal or vertical oval cross-section pipes placed in a cross stream. Int J Refrig 30:454–463. https://doi.org/10.1016/j.ijrefrig.2006.09.001

Chen WL, Dung WC (2008) Numerical study on heat transfer characteristics of double tube heat exchangers with alternating horizontal or vertical oval cross section pipes as inner tubes. Energy Convers Manag 49:1574–1583. https://doi.org/10.1016/j.enconman.2007.12.007

Chen WL, Guo Z, Chen CK (2004) A numerical study on the flow over a novel tube for heat-transfer enhancement with a linear Eddy-viscosity model. Int J Heat Mass Transf 47:3431–3439. https://doi.org/10.1016/j.ijheatmasstransfer.2004.01.014

Chen WL, Wong KL, Te HC (2006) A parametric study on the laminar flow in an alternating horizontal or vertical oval cross-section pipe with computational fluid dynamics. Int J Heat Mass Transf 49:287–296. https://doi.org/10.1016/j.ijheatmasstransfer.2005.07.005

Cheng J, Qian Z, Wang Q (2017) Analysis of heat transfer and flow resistance of twisted oval tube in low Reynolds number flow. Int J Heat Mass Transf 109:761–777. https://doi.org/10.1016/j.ijheatmasstransfer.2017.02.061

Chu P, He YL, Lei YG, Tian LT, Li R (2009) Three-dimensional numerical study on fin-and-oval-tube heat exchanger with longitudinal vortex generators. Appl Therm Eng 29:859–876. https://doi.org/10.1016/j.applthermaleng.2008.04.021

Du XP, Zeng M, Dong ZY, Wang QW (2014) Experimental study of the effect of air inlet angle on the air-side performance for cross-flow finned oval-tube heat exchangers. Exp Therm Fluid Sci 52:146–155. https://doi.org/10.1016/j.expthermflusci.2013.09.005

Elshazly E, Abdel-Rehim AA, El-Mahallawi I (2023) Thermal performance enhancement of evacuated tube solar collector using MWCNT, Al2O3, and hybrid MWCNT/ Al2O3nanofluids. Int J Thermofluids. 17:100260. https://doi.org/10.1016/j.ijft.2022.100260

Estel L, Bagui F, Abdelghani-Idrissi MA, Thenard C (2000) Distributed state estimation of a counter current heat exchanger under varying flow rate. Comput Chem Eng 24:53–60. https://doi.org/10.1016/S0098-1354(00)00301-X

Ghasemi H, Mozaffari S, Mousavi SH, Aghabarari B, Abu-Zahra N (2021) Decolorization of wastewater by heterogeneous Fenton reaction using MnO2-Fe3O4/CuO hybrid catalysts. J Environ Chem Eng 9:105091. https://doi.org/10.1016/J.JECE.2021.105091

Gholami A, Wahid MA, Mohammed HA (2017) Thermal–hydraulic performance of fin-and-oval tube compact heat exchangers with innovative design of corrugated fin patterns. Int J Heat Mass Transf 106:573–592. https://doi.org/10.1016/j.ijheatmasstransfer.2016.09.028

Gholami A, Mohammed HA, Wahid MA, Khiadani M (2019) Parametric design exploration of fin-and-oval tube compact heat

exchangers performance with a new type of corrugated fin patterns. Int J Therm Sci 144:173–190. https://doi.org/10.1016/j.ijthermalsci.2019.05.022

Herpe J, Bougeard D, Russeil S, Stanciu M (2009) Numerical investigation of local entropy production rate of a finned oval tube with vortex generators. Int J Therm Sci 48:922–935. https://doi.org/10.1016/j.ijthermalsci.2008.07.006

Insiat Islam RM, Hassan NMS, Rasul MG, Gudimetla PV, Nabi MN, Chowdhury AA (2023) Effect of non-uniform wall corrugations on laminar convective heat transfer through rectangular corrugated tube by using graphene nanoplatelets/MWCN hybrid nanofluid. Int J Therm Sci 187:108166. https://doi.org/10.1016/J.IJTHERMALSCI.2023.108166

Khanafer K, Vafai K (2011) A critical synthesis of thermophysical characteristics of nanofluids. Int J Heat Mass Transf 54:4410–4428. https://doi.org/10.1016/j.ijheatmasstransfer.2011.04.048

Kumar V, Saini S, Sharma M, Nigam KDP (2006) Pressure drop and heat transfer study in tube-in-tube helical heat exchanger. Chem Eng Sci 61:4403–4416. https://doi.org/10.1016/j.ces.2006.01.039

Liu S, Yin Y, Tu A, Zhu D (2020) Experimental investigation on shell-side performance of a novel shell and tube oil cooler with twisted oval tubes. Int J Therm Sci 152:106290. https://doi.org/10.1016/j.ijthermalsci.2020.106290

Mohammad AR, Nagaraju D, Kolla NK, Santhosi BVSRN (2022) Effective utilization of CuO/water nanofluid potential in the natural circulation loop. Int J Environ Sci Technol. https://doi.org/10.1007/s13762-021-03257-7

Nagaraju D, Mohammad AR, Santhosi BVSRN, Kolla NK, Tota RK (2023) Experimental and numerical analysis of convective heat transfer and entropy generation of graphene/water nanofluid in AEAOT heat exchanger. J Taiwan Inst Chem Eng. 150:105022. https://doi.org/10.1016/J.JTICE.2023.105022

Nagaraju D, Mohammad AR, Mendu SS, Uma MG (2024) Examining the potential of sigma-thermic heat transfer fluid and its nanofluid in a natural circulation loop through CFD studies. Eng Res Express 6:025540. https://doi.org/10.1088/2631-8695/AD4773

Rennie TJ, Raghavan VGS (2006) Numerical studies of a double-pipe helical heat exchanger. Appl Therm Eng 26:1266–1273. https://doi.org/10.1016/j.applthermaleng.2005.10.030

Sahu M, Sarkar J, Chandra L (2020) Transient thermo-hydraulics and performance characteristics of single-phase natural circulation loop using hybrid nanofluids. Int Commun Heat Mass Transf 110:104433. https://doi.org/10.1016/j.icheatmasstransfer.2019.104433

Sajadi AR, Yamani Douzi Sorkhabi S, Ashtiani D, Kowsari F (2014) Experimental and numerical study on heat transfer and flow resistance of oil flow in alternating elliptical axis tubes. Int J Heat Mass Transf. 77:124–30. https://doi.org/10.1016/j.ijheatmasstransfer.2014.05.014

Sajadi AR, Kowsary F, Bijarchi MA, Yamani Douzi Sorkhabi S (2016) Experimental and numerical study on heat transfer, flow resistance, and compactness of alternating flattened tubes. Appl Therm Eng. 108:740–50. https://doi.org/10.1016/j.applthermaleng.2016.07.033

Saleh B, Sundar LS (2021) Experimental study on heat transfer, friction factor, entropy and exergy efficiency analyses of a corrugated plate heat exchanger using Ni/water nanofluids. Int J Therm Sci 165:106935. https://doi.org/10.1016/j.ijthermalsci.2021.106935

Syam Sundar L, Said Z, Saleh B, Singh MK, Sousa ACM (2020) Combination of Co3O4 deposited rGO hybrid nanofluids and longitudinal strip inserts: thermal properties, heat transfer, friction factor, and thermal performance evaluations. Therm Sci Eng Prog 20:100695. https://doi.org/10.1016/j.tsep.2020.100695

Taler D, Ocłoń P (2014) Determination of heat transfer formulas for gas flow in fin-and-tube heat exchanger with oval tubes using CFD simulations. Chem Eng Process Process Intensif 83:1–11. https://doi.org/10.1016/j.cep.2014.06.011

Tan XH, Zhu DS, Zhou GY, Yang L (2013) 3D numerical simulation on the shell side heat transfer and pressure drop performances of twisted oval tube heat exchanger. Int J Heat Mass Transf 65:244–253. https://doi.org/10.1016/j.ijheatmasstransfer.2013.06.011

Tiwari S, Maurya D, Biswas G, Eswaran V (2003) Heat transfer enhancement in cross-flow heat exchangers using oval tubes and multiple delta winglets. Int J Heat Mass Transf 46:2841–2856. https://doi.org/10.1016/S0017-9310(03)00047-4

Tiwari AK, Ghosh P, Sarkar J (2013) Performance comparison of the plate heat exchanger using different nanofluids. Exp Therm Fluid Sci 49:141–151. https://doi.org/10.1016/j.expthermflusci.2013.04.012

Unger S, Beyer M, Szalinski L, Hampel U (2020) Thermal and flow performance of tilted oval tubes with novel fin designs. Int J Heat Mass Transf 153:119621. https://doi.org/10.1016/j.ijheatmasstransfer.2020.119621

Vaezi S, Karbalaee MS, Hanafizadeh P (2017) Effect of aspect ratio on heat transfer enhancement in alternating oval double pipe heat exchangers. Appl Therm Eng 125:1164–1172. https://doi.org/10.1016/j.applthermaleng.2017.07.070

Wang Y, Tian W, Ren J, Zhu L, Wang Q (2006) Influence of a building's integrated-photovoltaics on heating and cooling loads. Appl Energy 83:989–1003. https://doi.org/10.1016/j.apenergy.2005.10.002